IEEE Access
Multidisciplinary | Rapid Review | Open Access Journal

Received January 9, 2019, accepted January 28, 2019, date of publication March 26, 2019, date of current version April 10, 2019.

Digital Object Identifier 10.1109/ACCESS.2019.2903849

Compact Dominant Synergistic Excitation Pattern Learning for Illumination-Insensitive Image Representation With Boosting

TAO GAO, TING CHEN, C. C. WANG, ZHANWEN LIU, AND WEI LU, AND Y. H. LI
[1]School of Information Engineering, Chang'an University, Xi'an 710064, China

Corresponding authors: Ting Chen (tchenchd@126.com) and Y. H. Li (yhlichd@126.com)

This project is supported by the National Natural Science Foundation of China (61302150, 61703054), Fundamental Research Funds for the Central Universities, CHD (300102249314).

ABSTRACT Illumination-insensitive image representation is a great challenge in the computer vision field. Illumination variations considerably obstruct the effectiveness of image feature extraction. In this paper, we present a novel and generalized learning framework for illumination-insensitive image representation, which can learn the discriminative features through maximizing the inter-difference and minimizing intra-difference of the images with boosting. Particularly, we enhance the discriminative capacity of illumination-insensitive image representation in three aspects. First, we learn a subset of different synergistic Weber excitation patterns (SWEP) to generate the dominant SWEP (DSWEP) and DSWEP codebook for exploring optimal illumination-insensitive patterns. Second, a compact DSWEP (C-DSWEP) is learned with a boosted set of weight to generate C-DSWEP codebook. Discriminative learning is aimed at robustness and compactness. Third, the discriminative histogram learning model is established for encoding CDSEP to further improve the discriminative ability and reduce redundancy. The extensive experiments on CMUPIE, FERET, Yale B, Yale B ext., LFW, and PhoTex databases have highlighted the superiority and the robustness of our method compared with some other state-of-the-art methods.

INDEX TERMS Feature extraction, Weber law, feature learning, illumination variations.

I. INTRODUCTION

Illumination variations have imposed a much greater challenge on image representation. Image feature description has attracted tremendous attentions due to its great theoretical significance and broader practical applications, especially under complex illumination conditions, which mainly involves under exposure, over exposure and shadows [1], [2]. Face recognition in uncontrolled light variation conditions remains a challenging task [3]. most of current feature extraction methods are restricted to the conditions with good lighting whereas they probably fail to work under complex illumination conditions, e.g., images captured during nighttime or bad weather days [4]. It may cause the image either too dark or too bright, and then bias the face recognition algorithm [5]. Recently, to address these limitations caused by complex illumination, many methods have been extensively studied, mainly including three categories:

(i) Firstly, in the earlier time, some methods, based on reprocessing by equalization and normalization, are presented, such as histogram equalization (HE) [6], homomorphic filtering (HF) [7], logarithm transforms (LT) [8], local histogram specification (LHP) [9] and histogram specification (HS) [10], etc. These methods have manifested satisfactory performances under simple illumination condition, but due to the overly simplistic reprocessing, they always obtain inferior results in many real applications, especially under the complex illumination condition with multi-direction lightings.

(ii) In the second group, using transformation space theory, the methods mainly explore image feature extraction in certain lower-dimensional subspaces, which are robust to complex illumination variations, demonstrating superior performances over the past years. Among various

The associate editor coordinating the review of this manuscript and approving it for publication was Fan Zhang.

transformation methods, principal component analysis (PCA) [11] and its variants, i.e., kernel principal component analysis (KPCA) [10], block PCA [13], two dimensions PCA [14], incremental PCA [15] are well-known methods. Besides, considering the high-order statistic properties of samples, some typical methods are proposed, including independent components analysis (ICA) [16], linear discriminant analysis (LDA) [17], singular value decomposition (SVD) [18], discrete cosine transform (DCT) [19], Gabor transformation filters (GTF) [20], fisher vector (FV) [21], locally linear embedding (LLE) [22], wavelets [23] and Exclusive Vector quantization (ExVQ) [24] etc. However, these above methods can only work very well on the premise of enough available training samples as well as expensive computational cost, which are really some inevitable obstacles for real applications. Furthermore, all of them are holistic methods, which are easily sensitive to complex illumination and partial occlusion.

(iii) Methods of the third group mainly focus on exploiting the local illumination-insensitive features. In particular, local binary pattern (LBP) is the most representative one of local descriptors, proposed by Ojala *et al.* [25]. After that, many kinds of LBP variants are created, mainly including multi-resolution LBP [26], extended LBP (ELBP) [27], learning discriminative LBP (DLBP) [28], local quantized patterns (LQP) [29], local higher-order statistics (LHS) [30] and more. Since these methods cannot take full advantages of some direction information from local neighborhood, they always have limited performance in some degree. Thus, for overcoming this drawback, some further improved methods are presented, including local derivative pattern (LDP) [31], local Gabor XOR patterns (LGXP) [32], complete ELDP (CELDP) [33], eight local directional patterns (ELDP) [34], local directional number pattern (LDN) [35], adaptive homomorphic eight local directional patterns (AH-ELDP) [36], logarithmic fractal dimension (LFD) [37] and patterns of oriented edge magnitudes (POEM) [38], etc. Moreover, some method based on Gabor filters that mainly include local sub-Gabor (LG) [39], local Gabor textons (LGT) [40], histogram of Gabor phase patterns (HGPP) [41] and local Gabor binary pattern histogram sequence (LGBP) [42] have been proposed to achieve more favorable results due to their strong robustness to local distortions caused by illumination variance. These above methods have achieved favorable results. However, it's still hard to strip all the illumination components from images, or even impossible. Moreover, Methods focus on human visual perception are proposed to extract discriminative information from illumination images. Among various methods, Retinex transformation [43] and Weber local descriptors (WLD) [44] are the most popular ones. In addition, some modifications are presented, mainly including multi-scale Retinex (MSR) [45], facial landmarks and Weber local descriptor (FL-WLD) [46], Weber LBP (WLBP) [47] and self-quotient image (SQI) [48],generalized Weber-face (GWF) [49], patterns of Weber magnitude and orientation (PWMO) [50],high-order statistics of

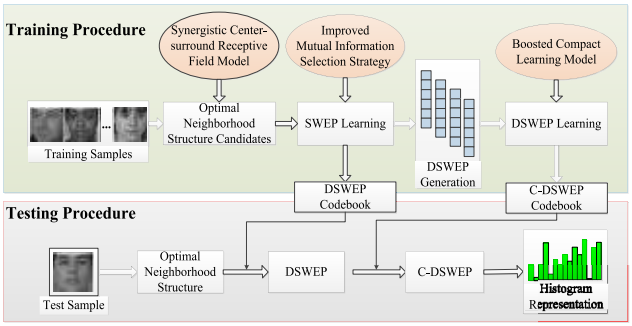

FIGURE 1. Pipeline of the proposed method.

Weber local descriptors (HOS-WLD) [51], robust discriminant regression (RDR) [52], polynomial contrast Binary Patterns (PCBP) [53], multilinear spatial discriminant analysis(MSDA) [54], Weber synergistic center-surround pattern (WSCP) [55] etc. Moreover, some other image enhancement methods [56], [57] are proposed. These above methods have demonstrated its superior capability. However, they still have some difficulties in fully utilizing excitations from neighborhood and almost all depend on handcraft.

Recently, learning mechanism has become a hot topic for discriminative feature extraction without handcraft and some representative algorithms are listed as follows: discriminant face descriptor (DFD) [58], compact binary face descriptor (CBFD) [59], bin boost [60],optimizing LBP [61], graph embedded extreme learning machine(GEELM) [62], selective regularized subspace learning (SRSL) [63] and more. Although more efficient, these learning methods emphasize the optimal weighting and selecting limited neighborhood in number and shape. Hence, how to select the optimal neighborhood structures to effectively represent local feature, how to exploit the discriminative and illumination-insensitive features to enlarge inter-difference and reduce intra-difference simultaneously and how to extract more compact binary feature are some critical and challenging problems remaining in pattern recognition.

In this paper, we propose a novel and generalized learning framework for illumination-insensitive feature representation. Generally, the generalized learning framework can be divided into three major steps, as depicted in Fig.1. We establish the optimal neighborhood structures based on synergistic center-surround receptive field model to provide richer candidates; and then an improved mutual information selection algorithm is proposed to learn the optimal DSWEP and generate the DSWEP codebook; moreover, we further learn the DSWEP using boosting compact learning model to exploit the compact and discriminative features, which are robustness to illumination and obtain C-DSWEP codebook. On the other hand, in the testing procedure, the final test image representation is acquired more effectively via both the DSWEP codebook and C-DSWEP codebook.

The main contributions of this paper are summarized as:

(i) Various optimal neighborhood structures and corresponding SWEPs, being robust to illumination variations, are

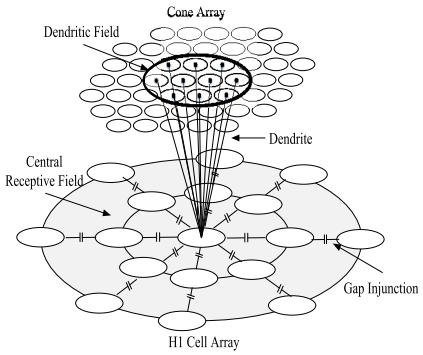

FIGURE 2. A schematic diagram of synergistic center-surround receptive field model for cell network.

produced to explore more effective and richer candidates for next step;

(ii) Different from the previous work, we propose a novel optimized information selection method to learn SWEP for according to criterion of minimizing redundancy and maximizing relevance and generate DSWEP codebook;

(iii) Boosting learning model is proposed to extract final feature C-DSWEP for further improving the discriminative ability of representation. Unlike the above methods, our learning frameworks can learn the optimal dominant structure as well as compact features in the form of sequence that associated with the weighting.

Structure of this paper is arranged as below: feature extraction background under complex illumination conditions and our main contributions are introduced in Section I; Our learning framework is described in Section II; Section III mainly conducts several relevant experiments and discusses the corresponding results; Finally, Section IV gives a brief summary of our work as well as the future expectations.

II. PROPOSED LEARNING FRAMEWORK

A. CANDIDATES OF SWEP

Packer *et al.* [64] propose a response model of neural cell, named as synergistic center-surround receptive field model, composed by horizontal cells network, which is shown in Fig.2. Inspired by this model, we establish a synergistic center-surround receptive field model to simulate the stimulus model of illumination image. As shown in Fig.3, the stimulus intensity of central pixel is affected by all of its surrounding neighbors with gap junctions, which can achieve strong response in active region while inhibits other inactive regions.

Motivated by this model, we firstly create a set of potential candidates of optimal neighborhood structures. The structure with 5×5 neighborhood has demonstrated its superior results over other neighborhood shapes [61]. Thus, in this paper, we adopt 5×5 neighborhood. In addition, based on Weber law [44], [49], different synergistic Weber excitation patterns are proposed for learning optimal neighborhood structures. Next, we define the different SWEP as:

$$\xi\left(m_0\right) = \arctan\left(\sum_{i=1}^{P} \frac{\Delta m_i}{m_0}\right) = \arctan\left(\frac{\Delta M}{m_0}\right) \tag{1}$$

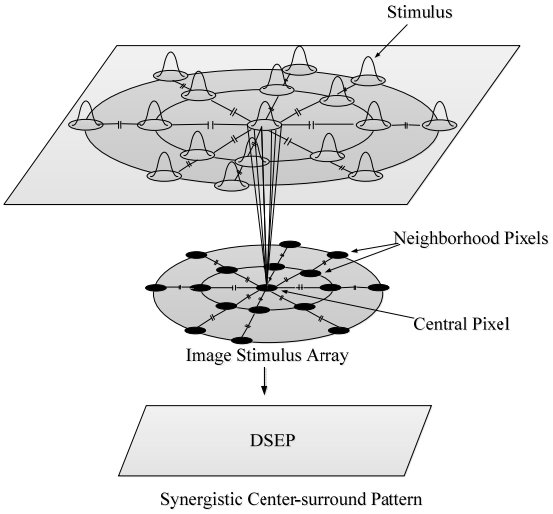

FIGURE 3. Synergistic center-surround receptive field model for image.

where m_0 is the value of central pixel; P is the number of neighboring pixels; and arctan () is the arctangent function. $\Delta m_i i = 1, 2, \cdots, P$ is defined in Eq. (2):

$$\Delta m_i = m_i - m_0 \tag{2}$$

In conventional WLD [44], [49], it only consider 8 neighboring pixels from the nearest layer. However, according to the synergistic center-surround receptive field model, central pixel's stimulus can be affected by the outer layer pixels as well as the inner layer pixels. Without loss of generality, we learn some dominant patterns to represent robust and discriminative features. In this paper, we set the number of candidate's neighboring pixels as 8. For preserving the hierarchical structure, we select the inner layer pixels set $(m_1, m_2, \cdots, m8)$ as one candidate and randomly choose 8 pixels from the outer layer m_j $(j = 9, \ldots, 24)$ as other candidate structures. Furthermore, to preferably describe the SWEP, we rewrite the Eq. (1) as:

$$\xi\left(I(x,y)\right) = \arctan\left(\frac{\alpha F'(I(x,y)) - \beta F_0(I(x,y))}{F_0(I(x,y))}\right) \tag{3}$$

where α and β are two coefficients to balance the weight distribution of central pixel and its neighboring pixels; $F_0\left(I(x,y)\right)$ and $F'\left(I(x,y)\right)$ denote the intensity sum of central and neighbor pixels respectively; and $I\left(x,y\right)$ is one pixel of image patch I. F_0 () and F' () should satisfy Eq. (4) and Eq. (5), respectively:

$$F_0\left(K * \left(I\left(x,y\right)\right)\right) = K * F_0\left(I\left(x,y\right)\right) \tag{4}$$

$$F'\left(K * \left(I\left(x,y\right)\right)\right) = K * F'\left(I\left(x,y\right)\right) \tag{5}$$

where K is a constant value .

According to the Retinex theory [43], [45], the image visual representation is composed by the distribution of source illumination and the object surface reflectance. In particular, the object surface information from our visual perception is determined by the reflectance component. Herein,

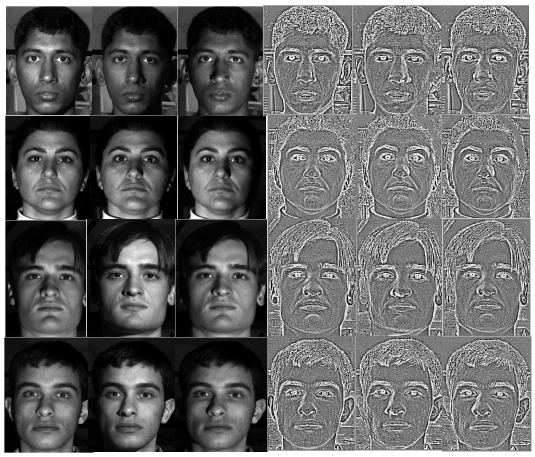

FIGURE 4. Some SWEP examples.

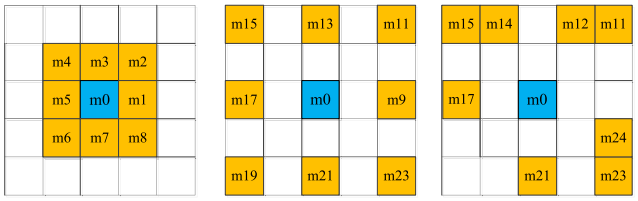

FIGURE 5. Some potential candidate structures. The candidate pixels are marked as yellow color and starting from 0 degree, their binarized pixel differences can be concatenated into a binary sequence in anti-clockwise.

an image can be described by Eq. (6):

$$I(x, y) = R(x, y) * L(x, y) \tag{6}$$

where $R(x, y)$ and $L(x, y)$ denote surface reflectance component and illumination component respectively. Substituting Eq. (6) to Eq. (3) gives:

$$\xi(I(x, y)) = \arctan\left(\frac{\alpha F'(R(x, y) * L(x, y)) - \beta F_0(R(x, y) * L(x, y))}{F_0(R(x, y) * L(x, y))}\right) \tag{7}$$

In a very small local region, the surface illumination components always change slowly and can be supposed to be a constant value. According to Eq. (4) and Eq. (5), Eq. (7) can be expressed as:

$$\begin{aligned}\xi(I(x, y)) &\approx \arctan\left(\frac{L(x, y) * \alpha F'(R(x, y)) - L(x, y) * \beta F_0(R(x, y))}{L(x, y) * F_0(R(x, y))}\right) \\ &= \arctan\left(\frac{\alpha F'(R(x, y)) - \beta F_0(R(x, y))}{F_0(R(x, y))}\right)\end{aligned} \tag{8}$$

As seen from Eq. (8), it is clear that SWEP is insensitive to illumination and can be utilized for representing the complex illumination image. Some SWEP of sample images are shown as Fig.4.

In general, we can acquire C_{16}^{8} candidate structures and partial structures of them are shown in Fig.5.

As seen from Eq. (8), the values of $\xi()$ is restricted to $[-\pi/2, \pi/2]$. In order to generate the corresponding histogram, the whole interval range $[-\pi/2, \pi/2]$ is equally segmented to N sub-intervals, marked as l_n $(n = 0, 1, \ldots, N-1)$ and defined in the following Eqs. (9) - (12):

$$l_n = \left[\eta_n^l, \eta_n^u\right] \tag{9}$$

$$\eta_n^l = (n/N - 1/2)\,\pi \tag{10}$$

$$\eta_n^u = ((n+1)/N - 1/2)\,\pi \tag{11}$$

$$n = \mathrm{mod}\left(\frac{\xi(x_c) + \pi/2}{\pi/N}, N\right) \tag{12}$$

where η_n^l and η_n^u are respectively the lower and upper limits of l_n. SWEP of image patch I is defined as:

$$H_n(I) = \sum_{x,y \in I} h(\xi(I(x, y)) \in l_n), \quad n = 0, 1, \ldots, N-1 \tag{13}$$

$$H(I) = \cup_{n=0}^{N-1} H_n(I) \tag{14}$$

where x and y denote the horizontal and vertical coordinates in an image patch I and function $h()$ is given:

$$h(X) = \begin{cases} 1 & X \text{ is true} \\ 0 & X \text{ is false} \end{cases} \tag{15}$$

For image patch I, SWEP of each candidate structure is marked as $f_r \in \mathbb{R}^N$, $(r = 1, 2, \cdots, R)$ where R is the number of candidates, which is shown as algorithm 1.

Algorithm 1 Candidates of SWEP

Input: image patch I;
Output: candidates of SWEP
1. **Initialization:** $H_{SWEP}^r \leftarrow \phi$;
2. **for** $r \leftarrow 1$ to R **do**
3. $\quad \xi^r(I(x, y)) \leftarrow \xi(I(x, y))$;
4. $\quad$ **for** $n \leftarrow 0$ to $N-1$ **do**
5. $\quad\quad H_n^r(I) \leftarrow \sum_{x,y \in I} h(\xi^r(I(x, y)) \in l_n)$;
6. $\quad$ **end for**
7. $\quad H^r(I) \leftarrow \cup_{n=0}^{N-1} H_n^r(I)$;
8. $\quad f_r \leftarrow H^r(I)$;
9. **end for**

B. LEARNING SWEP

Now we need to learn some dominant SWEPs to choose optimal neighborhood structures. According to the above analysis, for an image patch I, SWEPs of each candidate are marked as $f^r \in \mathbb{R}^N$, $(r = 1, 2, \cdots, R)$. In the learning phase, an optimized selection strategy using the improved mutual information (IMI) is proposed to learn SWEPs. The traditional mutual information (MI) [61], [65] methods have demonstrate its superior performance in feature selection aspect. MI [65] is the amount of information defined as:

$$I(f_k; f_t) = H(f_k) - H(f_k|f_t) \tag{16}$$

where f_t and f_k denote two given features; $H(f_k)$ and $H(f_k|f_t)$ are entropy and conditional entropy functions respectively.

The evaluation function $Score(f_t)$ of traditional MI is given by

$$Score(f_t) = \frac{1}{R}\sum_{r=1}^{R} I(f_r; f_t) = \frac{1}{R}\left(H(f_t) + \sum_{r=1, r\neq t}^{R} I(f_r; f_t)\right) \tag{17}$$

where R is the number of candidate features. In order to further utilize the class information, reduce redundancy and enlarge relevance, we suppose two functions: general relevance function $CS(f_t)$ and general redundancy function $CR(f_t)$ defined as in the Eq. (18) and Eq. (19):

$$CS(f_t) = \sum_{c=1}^{C} Score\left(f_t^c\right) \tag{18}$$

$$CR(f_t) = \sum_{c=1}^{C}\left(\frac{1}{D}\sum_{g_n^c \in G_D^c}\left(\left(1 - \frac{H(g_n^c|f_t^c)}{H(g_n^c)}\right) Score\left(g_n^c\right)\right)\right) \tag{19}$$

where C is the total class number, f_t^c is tth candidate of cth class. g_n^c and G_D^c denote the selected nth feature of cth class and its feature set with size of D. Thus, the improved evaluation function is proposed as:

$$U(f_t) = CS(f_t) - CR(f_t) \tag{20}$$

Next, let $G = [G^1, \cdots, G^C]$ denote the final set of the selected candidates and initialized as an empty set $\emptyset$. The first one of selected features $f_{\ell_1} = [f_{\ell_1}^1, \cdots, f_{\ell_1}^C]$ can be given by:

$$f_{\ell_1} = \arg\max_{1\le t\le R}\{CS(f_t)\} \tag{21}$$

We add f_{ℓ_1} into the set G as the first elements $g_1 = [g_1^1, \cdots, g_1^C]$. Similarly, other selected features f_{ℓ_2}, $f_{\ell_3}, \ldots, f_{\ell_D}$ are iteratively generated by:

$$U(f_t) = CS(f_t) - CR(f_t) \tag{22}$$

$$\ell_d = \arg\max_{1\le t\le R}\{U(f_t)\} \tag{23}$$

And then, $f_{\ell_2}, f_{\ell_3}, \ldots, f_{\ell_D}$ are added into the set G as elements $g_2, g_3, \ldots, g_D$, where D denote the number of optimal candidates. The selected features g_d, $(d = 1, 2, \cdots, D)$ corresponding sequence numbers in $f_r \in \mathbb{R}^N$, $r = 1, 2, \cdots, R$ are named as DSWEP vector $S^* \in \mathbb{R}^D$. The candidates $f_r^* \in \mathbb{R}^N, r \in S^*$ are formed as DSWEP codebook. The algorithm of learning SWEP is shown as algorithm 2.

Algorithm 2 Learning SWEP

Input: candidates of SWEP $f^r \in \mathbb{R}^N$, $r = 1, 2, \cdots, R$;
Output: dominant SWEP $f_r^* \in \mathbb{R}^N$, $r \in S^*$
1. **Initialization:** $G \leftarrow \phi$, $S^* \leftarrow \phi$;
2. **if** $d = 1$ **then**
3. **for** $r \leftarrow 1$ to R **do**
4. $f_{\ell_1} \leftarrow \arg\max\{CS(f_r)\}$;
5. **end for**
6. $g_1 \leftarrow f_{\ell_1}$;
7. $G \leftarrow g_1$;
8. **end if**
9. **for** $d \leftarrow 1$ **to** D **do**
10. **for** $r \leftarrow 1$ to R **do**
$\ell_d \leftarrow \arg\max\{U(f_t)\}$;
11. **end for**
12. $g_d \leftarrow f_{\ell_d}$;
13. $G \leftarrow g_d$;
14. **end for**
15. $S^* \in \mathbb{R}^D \leftarrow g_d$;
16. $f_r^* \in \mathbb{R}^N, r \in S^*$;

C. BOOSTING LEARNING DSWEP

The dimension of DSWEPs histogram is $N \times D \times B$ for an image if an image containing B patches. Thus, we adopt the DSWEP as weak learners and learn a descriptor to acquire C-DSWEP, inspired by boosted similarity sensitive coding [58]–[60]. We mark the weak learners $f_r^* \in \mathbb{R}^N, r \in S^*$ for image patch x as $Q(x) = (Q_1(x), Q_2(x), \cdots Q_D(x))$ where $Q_d(x) = f_r^*\big|_{r=1th}^{Dth} r \in S^* d = 1, 2, \cdots, D$ is a weak descriptor that can map the original representation x into K-dimension vectors.. The similarity measurement [66] of $Q(x)$ and $Q(y)$ is defined:

$$L(Q(x), Q(y)) = L_Q(x, y) \tag{24}$$

The exponential loss function between image patches is given by similarity measurement [60]:

$$\Gamma = \sum_{b=1}^{B} \exp\left(-\eta_b L_Q(x_b, y_b)\right) \tag{25}$$

where x_b, y_b are training image patches; B is the training patches number; $\eta_b \in \{1, -1\}$ is a coefficient whether (x_b, y_b) is an inter-class pair(1) or intra-class pair(-1). Our aim is to minimize the equation (25) for exploiting an embedding, maximizing the inter-difference and minimizing intra-difference of the images. The improved similarity measurement with boosting is presented as:

$$L_Q(x_b, y_b) = \sum_{k=1}^{D} LE(w_k^T Q(x_b), w_k^T Q(y_b)) \tag{26}$$

where K is the dimension of final vector and w_k is the weighted vector. $LE()$ is a function of loss.

Substituting $L_Q(x_b, y_b)$ in equation (25) gives

$$\Gamma = \sum_{b=1}^{B} \exp\left(-\gamma \eta_b \sum_{k=1}^{D} LE(w_k^T Q(x_b), w_k^T Q(y_b))\right) \tag{27}$$

Suppose the training sample set is

$$X = \{(x_1, y_1), (x_2, y_2), \ldots, (x_M, y_M)\} \tag{28}$$

where $y_i (i = 1, 2, \ldots, M)$ is the training sample label and M is the size of training sample set.

Firstly, the initial weight value of training sample is same as $1/M$. Moreover, the distribution of sample weight is set as

$$S_1(i) = (a_1, a_2, \ldots, a_M) = (\frac{1}{M}, \ldots, \frac{1}{M}) \tag{29}$$

Then, the DSWEP of each training sample is calculated and the new training sample set is established

$$X_k = \{(x_{k,1}, y_{k,1}), (x_{k,2}, y_{k,2}), \ldots, (x_{k,M}, y_{k,M})\} \tag{30}$$

Next, the training sample is tested using the weak learning and the label information is $h_k(x_{k,i})$, which indicate the predicted class label of *ith* training sample in the procedure of *kth*. The loss of iteration is calculated by distribution of sample weight

$$e_k = \sum_{i=1}^{M} a_{k,i}[h_k(x_{k,i}) \neq y_{k,i}] \tag{31}$$

where $a_{k,i}$ is the weight of *ith* training sample in the procedure of *kth*.

The classifier with minimum loss is set as the basic classifier in *kth* iteration and the weight of this classifier is

$$w_k = \frac{1}{2}\ln(\frac{1 - \min(e_k)}{\min(e_k)}) + \ln(c - 1) \tag{32}$$

where c is the number of class.

The distribution of sample weight is updated as

$$S_k(i) = S_{k-1}(i) \cdot \exp(\alpha_k \cdot [h_k(x_{k,i}) \neq y_{k,i}]) \tag{33}$$

Finally, the sample weight is normalized.

w_k is the weight of weak learners. Some details can be refer to [60].

The final feature is calculated as

$$Q(x) = (w_1 Q_1(x), w_2 Q_2(x), \cdots w_D Q_D(x)) \tag{34}$$

The algorithm of learning DSWEP is shown as algorithm 3.

Algorithm 3 Boosting Learning DSWEP

Input: DSWEP $f_r^* \in \mathbb{R}^N, r \in S^*$
Output: DSWEP weight w_k
1. **Initialization:** $w \leftarrow \phi, D_1(i) \leftarrow 1/M$
2. **for** $k \leftarrow 1$ **to** D **do**
3. **do for** $i \leftarrow 1$ **to** M **do**
4. **for** $d \leftarrow 1$ **to** D **do**
5. $e_d \leftarrow \sum_{t=1}^{m} a_{d,t}[h_1(x_{d,t}) \neq y_{d,t}]$
6. **end for**
7. $e_k = \min(e_1, e_2, \cdots, e_D)$
8. $w_k \leftarrow \frac{1}{2}\ln(\frac{1-e_k}{e_k}) + \ln(c-1)$;
9. $D_k(i) \leftarrow D_{k-1}(i) \cdot \exp(w_k \cdot [h_k(x_{k,i}) \neq y_{k,i}])$;
10. **end for**
11. **end for**

TABLE 1. Experimental environment setting.

Index	Environment	Configuration
1	Operation System	Window 7 with 64 bit
2	CPU	I7,2.5GHZ
3	Memory	4.0 G
4	Hard Disk	500 G
5	Program Design Tools	Matlab 2013b

III. COMPARISONS BY EXPERIMENTAL RESULTS

A. EXPERIMENT SETTING

Some comparative experiments have been conducted on several public image databases under complex illumination conditions including CMUPIE [68], Yale B [33], Yale B Ext [34], LFW [69], FERET [58] and PhoTex [70], [71]. There are six steps to evaluate our proposed method: firstly, the corresponding experiment setting is presented; next, we verify the effectiveness of the proposed method and discuss the effects of different parameter settings; then, Yale B and its Ext. databases are utilized to verify recognition accuracy under complex illuminations in the third part; after that, we also conduct some experiments on FERET database to test recognition accuracy; in the fifth part, LFW database is used to further validate the robustness to illumination variations; last, PhoTex database is adopted to examine methods with illumination-insensitive texture images.

The experimental environment settings are listed in Table 1.

B. PERFORMANCE EVALUATION OF THE PROPOSED C-DSWEP METHOD

In this section, we adopt CMUPIE database to evaluate comprehensive performance of the proposed method. The database contains images for 68 persons, each person under 13 different poses, 43 different illumination conditions, and with 4 different expressions. In this examination, half samples of each individual in different poses and illumination sub sets are selected randomly, which are adopted as the training collection. At the same time, the rest face images for each individual in different poses and illumination sub sets are adopted as the testing set.

1) GLOBAL C-DSWEP VS. LOCAL C-DSWEP

Local block scheme has been broadly applied to extract richer features [28], [58], [59]. Therefore, we divide one sample image into different sub-images and then, make local C-DSWEP learn from all of them, for the purpose of encoding the sample's final description. It is worth noting that different block schemes always have different effects on recognition result. Thus, we conduct several experiments with different block schemes, mainly including 1∗1, 2∗2, 4∗4, 6∗6, 8∗8, 12∗12 and multi (combination of 1∗1, 4∗4 and 8∗8) no overlapping regions separately. Let N = 16, $\alpha = 1$, $\beta = 1.25$, D = 4 and K = 64. Fig. 6 indicates the recognition rates with different block schemes. Performance will achieve a relevant

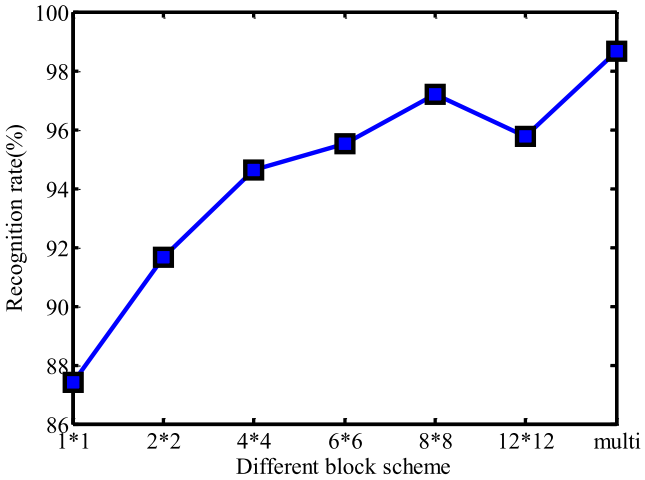

FIGURE 6. Recognition rate with different block schemes.

better result when with 8∗8 block scheme, and then become bad if the block numbers increase or decrease. Furthermore, the multi scheme can acquire the best performance for its capability of generating richer details, but inevitably sacrificing more computational costs.

2) CLARIFICATION ABOUT PARAMETERS α AND β

The parameters α and β are used to adjust the weighted values of central and adjacent stimulus. Let N $=$ 16, D $=$ 4 and K $=$ 64. The recognition rates with different parameters α and β are illustrated in Fig. 7, which indicates the superior performance of our proposed method if $\beta \geq \alpha$, especially $\beta = 1.25$ and $\alpha = 1$.

3) CLARIFICATION ABOUT PARAMETERS D AND K

Both D and K have an important effect on the learning procedures and results. The corresponding results reported in Fig. 8 reflect that the recognition rate will increase as D and K increase. Of course, the computational costs will inevitably increase. If balancing effectiveness with efficiency, C-DSWEP can achieve a relevant better result when K and D are respectively set to 64 and 4.

C. EXPERIMENTAL COMPARISON ON YALE B AND ITS EXTENDED DATABASES

To further evaluate the effectiveness of our proposed method under complex illumination conditions, Yale B and its extended database (Yale B Ext) are adopted. Yale B database has 10 subjects and each subject contains 576 viewing conditions, including 9 different poses and 64 different illumination conditions. Yale B Ext database is extent to 16,128 images for 38 individuals.

Similarly to the experimental settings in [33] and [34], we divide the images into five subsets according to light direction with respect to the camera axis. Final results reported in Fig. 9 manifest the method performances on Yale B database. It can be seen clearly that C-DSWEP achieves the best result when compared with WLD [44], GF [49], LBP [25], LDP [31],

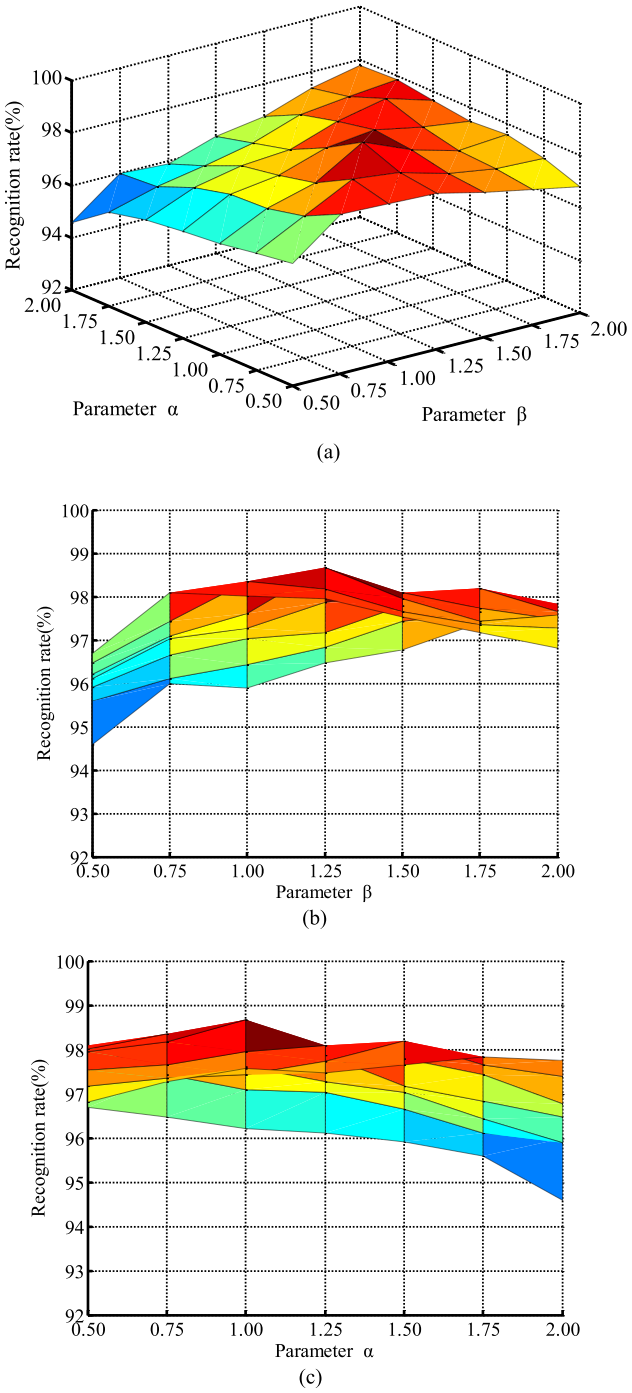

FIGURE 7. C-DSWEP performance with different parameters α and β. C-DSWEP performance with different parameters in 3D figure is shown in (a); C-DSWEP performance with different β and α are shown in (b) and (c).

ELDP [33], LDN [35] MW-SR [5] and MSDA [54]. The comparative average results between our proposed method and other existing methods are summarized in Table 2 on Yale B and Yale B Ext databases. C-DSWEP can really outperform WLD and WLBP by an interval of 4.73% and 5.21% respectively on Yale B database. For the reason that SWEP take full advantage of visual perception mechanism and utilize multi-layer model instead of single-layer of LBP, SWEP

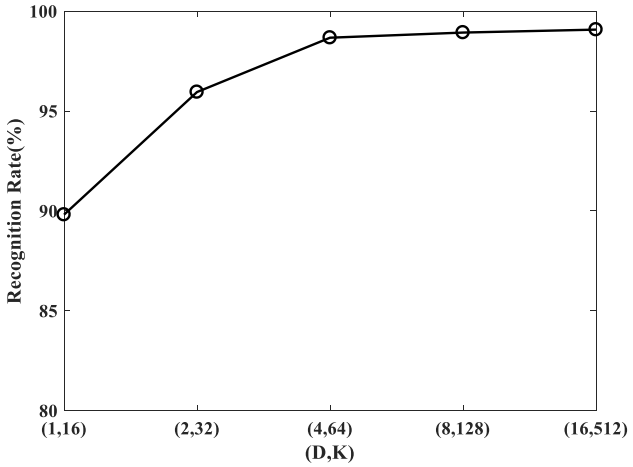

FIGURE 8. C-DSWEP performance with different parameters *K* and *D*.

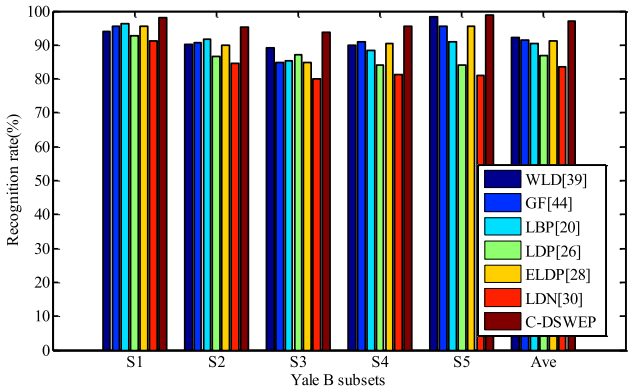

FIGURE 9. Performance comparisons on Yale B database.

can achieve the better recognition effect than traditional LBP and improve the recognition by an interval of 9.81%. It is worth noting that DWSEP learn the optimal SWEP candidates and improve SWEP to 94.07% on Yale B database. Next, C-DSWEP continue to optimize the performance of DSWEP and achieve the best results. Also, for the case of Yale B Ext, C-DSWEP also demonstrates its superior performance, which definitely verifies our original motivation in this paper.

D. EXPERIMENTAL COMPARISON ON FERET DATABASE

FERET database has 14,051 face images. There are some subsets in FERET database such as Fa, Fb, Fc, Dup1, Dup2, etc., which can be adopted to carry out some testes to further evaluate our proposed method.

We take Fa subset as the gallery set and other four standard testing protocols (Fb, Fc, dup I, dup II) with expression, pose, age and illumination variations as probe sets. In this experiment. The codebook size parameters D and K are set to 8 and 128. Finally, we implement the test to compare our method with other twelve state of art methods, including ELBP [27], DLBP [28], LQP [29], HGPP [41], FL-WLD [46], WLD [44], WLBP [47], PWMO [50], PCBP [53], WSCP [55] and more. The results reported in Table 3 indicate

TABLE 2. Performance comparisons on Yale B and Yale B Ext databases.

Descriptor	Yale B	Yale B Ext
Original	56.41	41.94
SQI [48]	66.25	45.31
GF [49]	91.11	78.76
WLD [44]	92.51	81.32
LBP [25]	89.68	73.44
WLBP [47]	92.03	80.79
LDP [31]	85.98	71.18
LDN [35]	95.13	82.91
LFD [37]	82.40	68.64
ELDP[33]	91.38	79.85
AH-ELDP[36]	96.67	85.77
MW-SR [5]	96.37	-
MSDA[54]	82.64	-
SWEP	92.21	83.25
DWSEP	94.07	86.73
C-DSWEP	**97.95**	**88.23**

TABLE 3. Performance comparisons on FERET database.

Descriptor	Fb	Fc	Dup1	Dup2
LDA[46]	31.0	28.5	36.3	42.3
LBP[25]	97.0	79.0	66.0	64.0
LGBP[42]	98	97	74	71
LGT[40]	97	90	71	67
LQP[29]	99.2	69.6	65.8	48.3
HGPP[41]	97.5	99.5	79.5	77.8
ELBP[27]	99.0	**100.00**	84.0	80.0
DLBP[28]	**99.6**	**100.00**	88.9	87.6
FL-WLD[46]	91.2	91.9	92.5	90.3
WLD[44]	80.1	75.5	89.8	89.7
WLBP[47]	97.0	96.0	77.0	71.6
PWMO[50]	94.0	99.0	82.0	81.0
PCBP[53]	94.8	98.5	78.5	73.5
WSCP[55]	97.6	93.2	92.1	89.8
C-DSWEP	99.3	99.5	**93.4**	**92.2**

that ELBP and DLBP can achieve the best recognition rate in literatures. Our proposed method can acquire almost the same results by only about 0.3%-0.5% differences in Fb and Fc subsets. On account of aiming at robustness to illumination variations, we mainly focus on the performance of our method under complex conditions in subsets Dup1 and Dup2. It is worth noting that C-DSWEP outperforms DLBP by an interval of 4.5% and 4.6%, and outperforms ELBP by an interval of 9.4% and 12.2%, respectively. In addition, our method also outperforms the second best method WSCP by an interval of 2.4% on set Dup2. In general, our proposed method can obtain superior performance on FERET database.

E. EXPERIMENTAL COMPARISON ON LFW DATABASE

For the sake of deeply evaluating the effectiveness of C-DSWEP in some real applications, we adopt Labeled Faces in the Wild (LFW) database, which is designed for studying

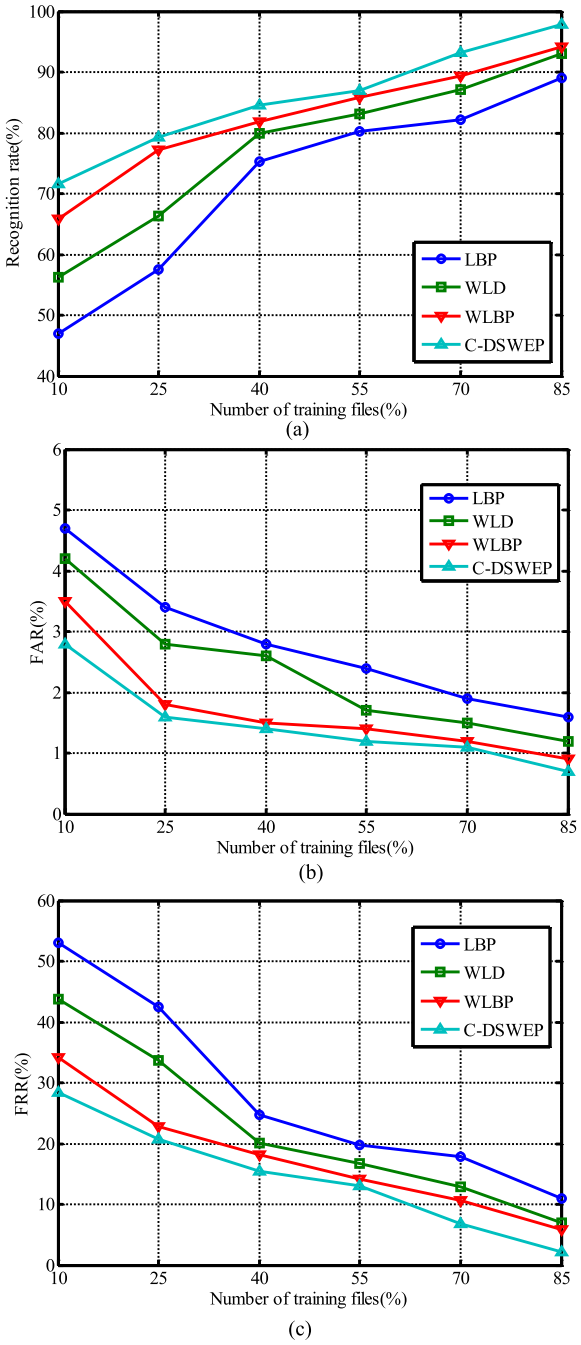

FIGURE 10. Performance comparisons on LFW database. (a) Recognition rate. (b) FAR. (c) FRR.

the problem of unconstrained face recognition. This data set contains more than 13,000 face images collected from the web. 1680 of the people pictured have two or more distinct photos in the data set. Here, we use the aligned images [69] and choose the individuals who have no less than 20 samples.

We evaluate the effectiveness of various methods via recognition rate, false acceptance rate (FAR) and false rejection rate (FRR). All comparative results are shown in Fig. 10, which reflect that, for all methods, the recognition rate will increase, and FAR and FRR will decrease, as the training number increases and become enough. In conclusion, our proposed method can achieve the best results across the number of training files, for the reason that C-DSWEP can utilize the most optimized model and extract more discriminative features compared with WLD and WLBP.

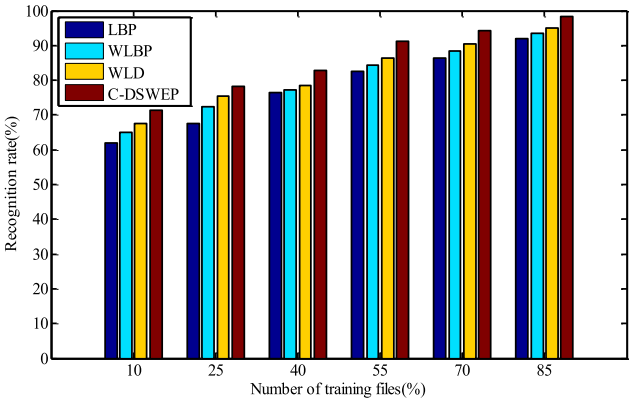

FIGURE 11. Performance comparisons on PhoTex database.

F. EXPERIMENTAL COMPARISON ON PHOTEX DATABASES

Through these above discussions, our method has achieved better performance in face databases. In order to further verify our methods in texture databases under complex illumination condition, we adopt PhoTex database [70], [71], which contains images of rough surfaces that have been illuminated from various directions. Images in this database are textures of various surfaces, which are placed on a fixed plane and are observed from a constant viewpoint for all different illumination directions. In this experiment, we choose 18 types of textures and each type has 20 captured images under complex illumination variations.

The results reported in Fig. 11 reflect that recognition rates of methods will increase as the training number increases and become enough. It is worth noting that C-DSWEP can acquire the best results across the number of training files for the same reason depicted in Section III E. In conclusion, C-DSWEP has the best robustness result under complex illumination variations not only in face feature representation aspect but also in texture feature description field.

IV. CONCLUSION

In this paper, we propose a novel and generalized learning framework for illumination-insensitive image representation with boosting, which can learn the discriminative features through maximizing the inter-difference and minimizing intra-difference of the images. We conduct abundant experiments to evaluate the effectiveness of our method on CMUPIE, FERET, Yale B, Yale B Ext and LFW databases. The results show that our method can demonstrate the superior performance not only in face feature representation aspect but also in texture feature description field. In the future study, we will continue to make further research to improve the proposed method and try to extend it in video-based face analysis.

REFERENCES

[1] H. Han, S. Shan, X. Chen, and W. Gao, "A comparative study on illumination preprocessing in face recognition," *Pattern Recognit.*, vol. 46, no. 6, pp. 1691–1699, Jun. 2013.

[2] J. W. Wang, N. T. Le, J. S. Lee, and C. C. Wang, "Illumination compensation for face recognition using adaptive singular value decomposition in the wavelet domain," *Inf. Sci.*, vol. 435, pp. 69–93, Apr. 2018.

[3] M. Smiatacz, "Normalization of face illumination using basic knowledge and information extracted from a single image," *Inf. Sci.*, vol. 469, pp. 14–29, Dec. 2018.

[4] C. Li, D. Song, R. Tong, and M. Tang, "Illumination-aware faster R-CNN for robust multispectral pedestrian detection," *Pattern Recognit.*, vol. 85, pp. 161–171, Jan. 2019.

[5] F. Cao, H. Hu, J. Lu, J. Zhao, Z. Zhou, and J. Wu, "Pose and illumination variable face recognition via sparse representation and illumination dictionary," *Knowl.-Based Syst.*, vol. 107, pp. 117–128, Sep. 2016.

[6] S. M. Pizer *et al.*, "Adaptive histogram equalization and its variations," *Comput. Vis., Graph., Image Process.*, vol. 39, no. 3, pp. 355–368, 1987.

[7] V. I. Voicu, R. Harley, R. Myler, and A. R. Weeks, "Practical considerations on color image enhancement using homomorphic filtering," *J. Electron. Imag.*, vol. 6, no. 1, pp. 108–113, 1997.

[8] M. Savvides and B. V. K. V. Kumar, "Illumination normalization using logarithm transforms for face authentication," in *Audio- and Video-Based Biometric Person Authentication*. Berlin, Germany: Springer, 2003, pp. 549–556.

[9] H.-D. Liu, M. Yang, and Y. Gao, "Local histogram specification for face recognition under varying lighting conditions," *Image Vis. Comput.*, vol. 32, no. 5, pp. 335–347, 2014.

[10] D. Coltuc, P. Bolon, and J.-M. Chassery, "Exact histogram specification," *IEEE Trans. Image Process.*, vol. 15, no. 5, pp. 1143–1152, May 2006.

[11] M. Kirby and L. Sirovich, "Application of the Karhunen–Loeve procedure for the characterization of human faces," *IEEE Trans. Pattern Anal. Mach. Intell*, vol. 12, no. 1, pp. 103–108, Jan. 1990.

[12] K. I. Kim, K. Jung, and H. J. Kim, "Face recognition using kernel principal component analysis," *IEEE Signal Process. Lett.*, vol. 9, no. 2, pp. 40–42, Feb. 2002.

[13] P.-C. Hsieh and P.-C. Tung, "A novel hybrid approach based on sub-pattern technique and whitened PCA for face recognition," *Pattern Recognit.*, vol. 42, no. 1, pp. 978–984, 2009.

[14] J. Yang and C. Liu, "Horizontal and vertical 2DPCA-based discriminant analysis for face verification on a large-scale database," *IEEE Trans. Inf. Forensics Security*, vol. 2, no. 4, pp. 781–792, Dec. 2007.

[15] D. Huang, Z. Yi, and X. Pu, "A new incremental PCA algorithm with application to visual learning and recognition," *Neural Process. Lett.*, vol. 30, no. 3, pp. 171–185, 2009.

[16] Z.-L. Sun and K.-M. Lam, "Depth estimation of face images based on the constrained ICA model," *IEEE Trans. Inf. Forensics Security*, vol. 6, no. 2, pp. 360–370, Jun. 2011.

[17] Z. Liu, J. Zhou, and Z. Jin, "Face recognition based on illumination adaptive LDA," in *Proc. 20th Int. Conf. Pattern Recognit. (ICPR)*, Istanbul, Turkey, 2010, pp. 894–897.

[18] W. Kim, S. Suh, J.-J. Han, and W. Hwang, "SVD face: Illumination-invariant face representation," *IEEE Signal Process. Lett.*, vol. 21, no. 11, pp. 1336–1340, Nov. 2014.

[19] W. Chen, M. J. Er, and S. Wu, "Illumination compensation and normalization for robust face recognition using discrete cosine transform in logarithm domain," *IEEE Trans. Syst. Man, Cybern. B, Cybern.*, vol. 36, no. 2, pp. 458–466, Apr. 2006.

[20] M. Yang, L. Zhang, S. C. K. Shiu, and D. Zhang, "Gabor feature based robust representation and classification for face recognition with Gabor occlusion dictionary," *Pattern Recognit.*, vol. 46, no. 7, pp. 1865–1878, Jul. 2013.

[21] K. Simonyan, O. M. Parkhi, A. Zisserman, and A. Vedaldi, "Fisher Vector Faces in the Wild," *BMVC*, 2013, vol. 5, no. 6, p. 11.

[22] S. T. Roweis and L. K. Saul, "Nonlinear dimensionality reduction by locally linear embedding," *Science*, vol. 290, no. 5500, pp. 2323–2326, Dec. 2000.

[23] H. Hu, "Illumination invariant face recognition based on dual-tree complex wavelet transform," *IET Comput. Vis.*, vol. 9, no. 2, pp. 163–173, 2015.

[24] Y. Zhang, J. Wu, and W. Lin, "Exclusive visual descriptor quantization," in *Proc. Asian Conf. Comput. Vis. (ACCV)*, 2012, pp. 408–421.

[25] T. Ojala, M. Pietikäinen, and T. Mäenpää, "A generalized local binary pattern operator for multiresolution gray scale and rotation invariant texture classification," in *Advances in Pattern Recognition—ICAPR* (Lecture Notes in Computer Science). Heidelberg, Germany: Springer, 2001, pp. 397–406.

[26] T. Ojala, M. Pietikainen, and T. Maenpaa, "Multi resolution gray-scale and rotation invariant texture classification with local binary patterns," *IEEE Transactions on Pattern Analysis and Machine Intelligence*, vol. 24, no. 7, pp. 971–987, 2002.

[27] L. Liu, P. Fieguth, M. Pietikäinen, D. Hu, and G. Zhao, "Extended local binary patterns for face recognition," *Inf. Sci.*, vols. 358–359, pp. 56–72, Sep. 2016.

[28] D. Maturana, D. Mery, and A. Soto, "Learning discriminative local binary patterns for face recognition," in *Proc. IEEE Int. Conf. Autom. Face Gesture Recognit. Workshops (FG)*, Mar. 2011, pp. 470–475.

[29] S. Hussain, T. Napoléon, and F. Jurie, "Face recognition using local quantized patterns," in *Proc. Conf. Brit. Machive Vis.*, 2012, p. 11.

[30] G. Sharma, S. ul Hussain, and F. Jurie, "Local higher-order statistics (LHS) for texture categorization and facial analysis," in *Computer Vision—ECCV*. Berlin, Germany: Springer, 2012, pp. 1–12.

[31] B. Zhang, Y. Gao, S. Zhao, and J. Liu, "Local derivative pattern versus local binary pattern: Face recognition with high-order local pattern descriptor," *IEEE Trans. Image Process.*, vol. 19, no. 2, pp. 533–544, Feb. 2010.

[32] S. Xie, S. Shan, X. Chen, and J. Chen, "Fusing local patterns of Gabor magnitude and phase for face recognition," *IEEE Trans. Image Process.*, vol. 19, no. 5, pp. 1349–1361, May 2010.

[33] M. R. Faraji and X. Qi, "Face recognition under varying illuminations using logarithmic fractal dimension-based complete eight local directional patterns," *Neurocomputing*, vol. 199, pp. 16–30, Jul. 2016.

[34] M. R. Faraji and X. Qi, "Face recognition under illumination variations based on eight local directional patterns," *IET Biometrics*, vol. 4, no. 1, pp. 10–17, 2015.

[35] A. Ramirez Rivera, R. Castillo, and O. Chae, "Local directional number pattern for face analysis: Face and expression recognition," *IEEE Trans. Image Process.*, vol. 22, no. 5, pp. 1740–1752, May 2013.

[36] M. R. Faraji and X. Qi, "Face recognition under varying illumination based on adaptive homomorphic eight local directional patterns," *IET Comput. Vis.*, vol. 9, no. 3, pp. 390–399, 2014.

[37] M. R. Faraji and X. Qi, "Face recognition under varying illumination with logarithmic fractal analysis," *IEEE Trans. Signal Process. Lett.*, vol. 21, no. 12, pp. 1457–1461, Dec. 2014.

[38] N.-S. Vu and A. Caplier, "Enhanced patterns of oriented edge magnitudes for face recognition and image matching," *IEEE Trans. Image Process.*, vol. 21, no. 3, pp. 1352–1365, Mar. 2012.

[39] H. R. Kanan and K. Faez, "Recognizing faces using Adaptively Weighted Sub-Gabor Array from a single sample image per enrolled subject," *Image Vis. Comput.*, vol. 28, no. 3, pp. 438–448, 2010.

[40] Z. Lei, S. Z. Li, X. Zhu, and R. Chu, "Face recognition with local Gabor textons," in *Advances in Biometrics*. Berlin, Germany: Springer, 2007, pp. 49–57.

[41] B. Zhang, S. Shan, X. Chen, and W. Gao, "Histogram of Gabor phase patterns (HGPP): A novel object representation approach for face recognition," *IEEE Trans. Image Process.*, vol. 16, no. 1, pp. 57–68, Jan. 2007.

[42] W. Zhang, S. Shan, X. Chen, H. Zhang, and W. Gao, "Local Gabor binary pattern histogram sequence (LGBPHS): A novel non-statistical model for face representation and recognition," in *Proc. 10th IEEE Int. Conf. Comput. Vis.(ICCV)*, vol. 1, Oct. 2005, pp. 786–791.

[43] E. H. Land, "Recent advances in Retinex theory," *Vis. Res.*, vol. 26, no. 1, pp. 7–21, 1986.

[44] J. Chen *et al.*, "WLD: A robust local image descriptor," *IEEE Trans. Pattern Anal. Mach. Intell.*, vol. 32, no. 9, pp. 1705–1720, Sep. 2010.

[45] Z. Rahman, D. J. Jobson, and G. A. Woodell, "Multi-scale retinex for color image enhancement," in *Proc. IEEE Int. Conf. Image Process.*, vol. 3, Sep. 1996, pp. 1003–1006.

[46] Z. Zhang, L. Wang, S.-K. Chen, Y. Chen, and Q. Zhu, "Pose-invariant face recognition using facial landmarks and Weber local descriptor," *Knowl.-Based Syst.*, vol. 84, pp. 78–88, Aug. 2015.

[47] F. Liu, Z. Tang, and J. Tang, "WLBP: Weber local binary pattern for local image description," *Neurocomputing*, vol. 120, pp. 325–335, Nov. 2013.

[48] H. Wang, S. Z. Li, Y. Wang, and J. Zhang, "Self quotient image for face recognition," in *Proc. IEEE Int. Conf. Image Process.*, vol. 2, Oct. 2004, pp. 1397–1400.

[49] Y. Wu, Y. Jiang, W. Li, Z. Lu, Q. Liao, and Y. Zhou, "Generalized Weber-face for illumination-robust face recognition," *Neurocomputing*, vol. 136, pp. 262–267, Jul. 2014.
[50] Y. Jiang, B. Wang, W. Li, Q. Liao, and Y. Zhou, "Patterns of Weber magnitude and orientation for uncontrolled face representation and recognition," *Neurocomputing*, vol. 165, pp. 190–201, Oct. 2015.
[51] X.-H. Han, Y.-W. Chen, and G. Xu, "High-order statistics of Weber local descriptors for image representation," *IEEE Trans. Cybern.*, vol. 45, no. 6, pp. 1180–1193, Jun. 2015.
[52] Z. Lai, D. Mo, W. K. Wong, Y. Xu, D. Miao, and D. Zhang, "Robust discriminant regression for feature extraction," *IEEE Trans. Cybern.*, vol. 48, no. 8, pp. 2472–2484, Aug. 2018.
[53] Z. Xu, Y. Jiang, Y. Wang, Y. Zhou, W. Li, and Q. Liao, "Local polynomial contrast binary patterns for face recognition," *Neurocomputing*, to be published. doi: 10.1016/j.neucom.2018.09.056.
[54] S. Yuan, X. Mao, and L. Chen, "Multilinear spatial discriminant analysis for dimensionality reduction," *IEEE Trans. Image Process.*, vol. 26, no. 6, pp. 2669–2681, Jun. 2017.
[55] G. Tao, X. Zhao, T. Chen, Z. Liu, and S. Li, "Illumination-insensitive image representation via synergistic weighted center-surround receptive field model and Weber law," *Pattern Recognit.*, vol. 69, pp. 124–140, Sep. 2017.
[56] Y. Chen, W. Lin, C. Zhang, Z. Chen, N. Xu, and J. Xie, "Intra-and-inter-constraint-based video enhancement based on piecewise tone mapping," *IEEE Trans. Circuits Syst. Video Technol.*, vol. 23, no. 1, pp. 74–82, Jan. 2013.
[57] L. Xie, J. Wang, W. Lin, B. Zhang, Q. Tian, "Towards reversal-invariant image representation," *Int. J. Comput. Vis.*, vol. 123, no. 2, pp. 226–250, 2017.
[58] Z. Lei, M. Pietikäinen, and S. Z. Li, "Learning discriminant face descriptor," *IEEE Trans. Pattern Anal. Mach. Intell.*, vol. 36, no. 3, pp. 289–302, Feb. 2014.
[59] J. Lu, V. E. Liong, X. Zhou, and J. Zhou, "Learning compact binary face descriptor for face recognition," *IEEE Trans. Pattern Anal. Mach. Intell.*, vol. 37, no. 10, pp. 2041–2056, Oct. 2015.
[60] T. Trzcinski, M. Christoudias, and V. Lepetit, "Learning image descriptors with boosting," *IEEE Trans. Pattern Anal. Mach. Intell.*, vol. 37, no. 3, pp. 597–610, Mar. 2015.
[61] J. Ren, X. Jiang, J. Yuan, and G. Wang, "Optimizing LBP structure for visual recognition using binary quadratic programming," *IEEE Signal Process. Lett.*, vol. 21, no. 11, pp. 1346–1350, Nov. 2014.
[62] A. Iosifidis, A. Tefas, and I. Pitas, "Graph embedded extreme learning machine," *IEEE Trans. Cybern.*, vol. 46, no. 1, pp. 311–324, Jan. 2016.
[63] C. Luo, B. Ni, S. Yan, and M. Wang, "Image classification by selective regularized subspace learning," *IEEE Trans. Multimedia*, vol. 18, no. 1, pp. 40–50, Jan. 2016.
[64] O. S. Packer and D. M. Dacey, "Synergistic center-surround receptive field model of monkey H1 horizontal cells," *J. Vis.*, vol. 5, no. 11, pp. 9–18, 2005.
[65] X. Junling *et al.*, "An unsupervised feature selection approach based on mutual information," in *J. Comput. Res. Develop.*, vol. 49, no. 2, pp. 372–382, 2012.
[66] G. Shakhnarovich, "Learning task-specific similarity," Ph.D. dissertation, Dept. Elect. Eng. Comput. Sci., MIT, Cambridge, MA, USA, 2006.
[67] A. Torralba, R. Fergus, and Y. Weiss, "Small codes and large image databases for recognition," in *Proc. IEEE Conf. Comput. Vis. Pattern Recognit.*, Jun. 2008, pp. 1–8.
[68] T. Sim, S. Baker, and M. Bsat, "The CMU pose, illumination, and expression (PIE) database," in *Proc. 5th IEEE Int. Conf. Autom. Face Gesture Recognit.*, May 2002, pp. 46–51.
[69] G. Huang, M. Mattar, H. Lee, and E. G. Learned-Miller, "Learning to align from scratch," in *Adv. Neural Inf. Process. Syst.*, 2012, pp. 764–772.
[70] M. Jian, K.-M. Lam, and J. Dong, "Illumination-insensitive texture discrimination based on illumination compensation and enhancement," *Inf. Sci.*, vol. 269, pp. 60–72, Jun. 2014.
[71] M. Chantler, "The PhoTex database," Texture Lab., Heriot-Watt Univ. Edinburgh, Edinburgh, U.K. [Online]. Available: http://www.macs.hw.ac.uk/texturelab /resources/databases/

Authors' photographs and biographies not available at the time of publication.